Self-consistent electronic states for reconstructed Si vacancy models*

Steven G. Louie,† M. Schlüter,‡ James R. Chelikowsky, and Marvin L. Cohen
Department of Physics, University of California
and Inorganic Materials Research Division, Lawrence Berkeley Laboratory, Berkeley, California 94720
(Received 2 October 1975)

Vacancy states in Si are investigated using a recently developed self-consistent pseudopotential technique. Three different structural models (ideal and two reconstructions) for a neutral vacancy are considered. Vacancy states are found to exist in the Si thermal gap for each structure. The character of these states is predominantly dangling-bond p-like localized on the four atoms surrounding the vacancy. The ideal (unreconstructed) vacancy yields an electronic spectrum, which is unstable with respect to Jahn-Teller type distortions. The two different reconstruction models considered yield Jahn-Teller stable situations.

I. INTRODUCTION

Despite numerous theoretical investigations, the detailed electronic structure of deep defect states in semiconductors remains essentially an unsolved problem.[1] The main difficulties arise from the fact that deep levels in the semiconductor gap imply a strongly localized defect potential often combined with structural reconstruction in the vicinity of the defect. Consider the case of an isolated neutral vacancy (V^0) in Si. Several different methods of calculation have been employed leading to quite different results. Among them defect molecule calculations[2,3] have provided only qualitative information about the Si vacancy levels; as of yet no connection with the band structure has been established. Results from one-electron methods using clusters of Si atoms such as the extended Hückel method strongly depend on the size of the cluster, the basis functions used, and the boundary conditions imposed.[4,5] Finally, studies considering the vacancy as a perturbation on the perfect Si crystal give results ranging from having only resonant vacancy states in the Si conduction band[6] to having localized states anywhere in the forbidden gap depending on an arbitrary scaling of the perturbing vacancy pseudopotential.[7]

Experimentally the energy levels for the *neutral* vacancy (V^0) in Si are not well determined. However, they are believed to be deep (at least a few tenths of an eV) in the forbidden gap.[8,9] Moreover, from electron paramagnetic measurements,[8] it is found that both the singly positive (V^+) and negative (V^-) charged states of the Si vacancy undergo a structural reconstruction. For the V^+ state, a tetragonal Jahn-Teller distortion is observed; and for the V^- state, a mixed tetragonal and trigonal distortion is found. A similar type of reconstruction is expected for the V^0 state.

In this paper the electronic structure of a neutral vacancy in Si is studied using a recently developed method involving self-consistent pseudopotentials.[10] To study the effect of local reconstruction we have considered three different structural models for the Si vacancy: the ideal undisturbed structure and two differently reconstructed structures. Self-consistency in the present context means the self-consistent electronic response to a given structural model. Among the above-mentioned methods for calculating the electronic properties of a semiconductor vacancy, only the defect molecule calculations are self-consistent in this spirit. To our knowledge, the present work is the first calculation of a Si vacancy in which bulk band-structure effects are included and which at the same time is self-consistent.

In the present calculations, the lattice vacancies are repeated periodically to form a superlattice of vacancies embedded in the infinite Si crystal and the electronic structure of this periodic system is calculated self-consistently.[11] Hence the vacancy levels are spread into bands with dispersion in $\vec{k}$ space. The amount of dispersion provides a measure of the localization of the vacancy states. It is found that localized vacancy states in the gap and strong resonant states in the valence band existed for the three structural models. The characteristics of these states have been studied by analyzing their charge densities. In addition, a tight-binding model has been fitted to the vacancy bands for the ideal case. From the fitted tight-binding parameters, the "dispersionless" energies of vacancy levels which correspond to isolated vacancies can be extracted.

The remainder of the paper is organized as follows: In Sec. II the steps in the self-consistent calculations and the tight-binding model are discussed. In Sec. III the results for the electronic structure of the Si neutral vacancy for three structural models are presented and discussed. In Sec. IV some conclusions are presented.

II. CALCULATIONS

In this section a description is given of the self-consistent calculations, carried out for the

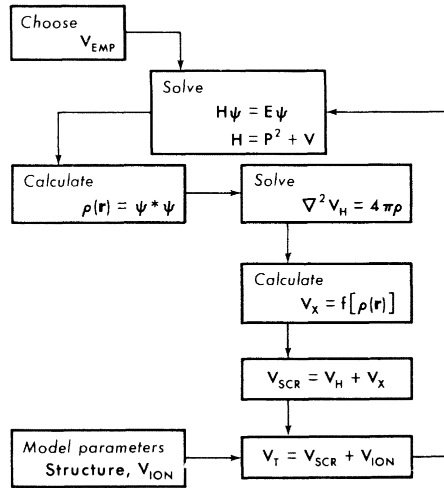

FIG. 1. Block diagram of the computational steps in achieving a self-consistent screening potential in response to a given structural model.

three structural models of the neutral Si vacancy. In addition a tight-binding model used to fit the vacancy bands for the ideal vacancy is presented.

A. Self-consistent pseudopotential calculations

As mentioned in Sec. I, the method employed here for the calculation of a local configuration consists of periodically repeating the particular local configuration to form a superlattice. Self-consistent pseudopotentials are then used to compute the electronic structure. The steps leading to a self-consistent solution to the vacancy problem are schematically shown in Fig. 1. The method has been applied successfully to the calculation of a Si diatomic molecule[10] and to the calculations of crystalline surfaces[12–14] and solid interfaces.[15] A detailed discussion of the method has been given in Ref. 13 and 15; it therefore will only be briefly described below.

Two essential features of the method are: (a) Self-consistency in the potential is required to allow for the correct electronic screening around the vacancy site and (b) periodicity is retained artificially which permits the use of standard pseudopotential techniques.

For the present case of a Si vacancy, the infinite Si crystal is divided into large fcc unit cells each containing 54 atoms. Neutral vacancies are simulated by removing an identical atom from each cell. The different structural models involve different reconstructions for the positions of the atoms surrounding the vacancy site. Test runs with various cell sizes indicated that at least 54-atom unit cells are needed to quantitatively provide the essential physics of the system. In the 54-atom unit cell neighboring vacancies are separated by six Si–Si bonds. The self-consistent loop (see Fig. 1) is initiated with an empirical pseudopotential carried over from crystalline calculations. From the resulting total charge density, a Hartree screening potential and an exchange potential of the Slater type are derived and added to an atomic Si^{+4} ion pseudopotential to form a new total pseudopotential for the next iteration. New screening and exchange potentials are derived and the process is repeated until self-consistency (stability of input vs output potentials within 0.005 Ry) is reached.

The self-consistent cycle is initiated using the following starting potential:

$$V_{\text{start}}(\vec{G}) = S(\vec{G}) V^{\text{Si}}_{\text{emp}}(|\vec{G}|) \ , \tag{1}$$

where $\vec{G}$ are reciprocal-lattice vectors and the Si structure factor

$$S(\vec{G}) = \frac{1}{M} \sum_{\vec{\tau}_i}^{M} e^{-i\vec{G}\cdot\vec{\tau}_i} \tag{2}$$

describes the positions of the atoms in the large 54-atom unit cell. $V^{\text{Si}}_{\text{emp}}(|\vec{G}|)$ are the Si atomic pseudopotential form factors fitted to empirical bulk calculations.[16] They are derived from a continuous extrapolation of the form

$$V^{\text{Si}}_{\text{emp}}(q) = \frac{a_1(q^2 - a_2)}{\exp[a_3(q^2 - a_4)] + 1} \ , \tag{3}$$

where the four parameters a_i are given in Table I. The potential $V^{\text{Si}}_{\text{emp}}(q)$ is normalized to an atomic volume of 137.6 (a.u.)^3 with units of Ry if q is entered in a.u. Using this starting potential, the band structure $E_n(\vec{k})$ and the wave functions $\psi_{n\vec{k}}(\vec{r})$ can then be calculated using standard methods,[17] i.e., expanding the electron wave function in plane waves with reciprocal-lattice vectors and diagonalizing the Hamiltonian matrix to obtain electronic energy $E_n(\vec{k})$ and the electronic wave function $\psi_{n\vec{k}}$.

To perform the next step in the self-consistent loop, the total valence charge density

$$\rho(\vec{r}) = \sum_{\vec{k}} \rho_{\vec{k}}(\vec{r}) = 2 \sum_{\vec{k}} \sum_{n} |\psi_{n\vec{k}}(\vec{r})|^2 \tag{4}$$

has to be evaluated. There are 106 occupied bands in the band-structure scheme (no spin-orbit in-

TABLE I. Form-factor parameters for the empirical Si pseudopotential V_{emp} [Eq. (3)] and for the ionic Si^{4+} pseudopotential V_{ion} [Eq. (8)].

V_{emp}	V_{ion}
$a_1 = 0.342\,70$	$b_1 = -1.125\,07$
$a_2 = 2.221\,44$	$b_2 = 0.790\,65$
$a_3 = 0.863\,34$	$b_3 = -0.352\,01$
$a_4 = 1.534\,57$	$b_4 = -0.018\,07$

teraction). For reasonable convergence of the wave functions, a matrix size of the order of 750×750 is needed when the Hamiltonian is expanded in plane waves. This corresponds to a kinetic energy cutoff[17] $E_1=|\vec{G}^2_{max}|\approx 2.7$ Ry. In addition, another ~800 plane waves were included via Löwdin's perturbation scheme[17] to further improve the accuracy of the eigenenergies. To avoid a full Brillouin zone evaluation of the total charge density at each iteration of the self-consistent process, the total charge density $\rho(\vec{r})$ is approximated by the charge density evaluated at one point $\vec{k}=\Gamma$. The point Γ was chosen because, among the high-symmetry points, $\rho_\Gamma(\vec{r})$ provides a good representation of $\rho(\vec{r})$ for crystalline Si. At the bond and atomic sites, $\rho_\Gamma(\vec{r})$ of bulk Si is within 10% of the charge density given by a full zone calculation. The choice of high-symmetry points is necessary because the Hamiltonian matrix can then be reduced by using symmetrized plane waves.

Once $\rho(\vec{r})$ is known, the Hartree screening potential V_H and the Hartree-Fock-Slater exchange potential V_x are evaluated using

$$V_H(\vec{G})=\frac{4\pi e^2\rho(\vec{G})}{|\vec{G}|^2} \tag{5}$$

$$V_x(\vec{G})=-\alpha(3/2\pi)(3\pi^2)^{1/3}e^2\rho^{1/3}(\vec{G}) \ , \tag{6}$$

where $\alpha=0.79$ and $\rho(\vec{G})$ and $\rho^{1/3}(\vec{G})$ are the Fourier components of $\rho(\vec{r})$ and $\rho^{1/3}(\vec{r})$, respectively. Justification for the use of the Slater exchange potential and the choice of α are discussed in detail in Ref. 13. V_H and V_x together form the electronic screening potential of the system. They are then added to an ionic potential

$$V_{ion}(\vec{G})=S(\vec{G})\,V^{Si}_{ion}(\vec{G}) \tag{7}$$

to form an input potential for the next iteration. For V^{Si}_{ion}, we have used a local approximation of a Abarenkov-Heine atomic model potential[18] which is fitted to the following four-parameter potential

$$V^{Si}_{ion}(q)=(b_1/q^2)\,[\cos(b_2q)+b_3]e^{b_4q^4}. \tag{8}$$

The values of the b_i's are given in Table I. The normalization and the units for Eq. (8) are the same as those for Eq. (3).

The calculation is continued by repeating the whole cycle. However, owing to the divergent character of V_H and V_{ion} for small $\vec{G}$'s, self-consistency cannot be achieved straightforwardly by using the output screening potential from one iteration as the input screening potential for the next iteration.[19] An alternative procedure to the one suggested in Ref. 13 is used in the present calculations. The input screening potential of the nth iteration is taken to be a weighted linear combination of the input and output screening potentials of the $(n-1)^{th}$ iteration. The criterion for self-consistency is the stability of the subsequent output screening potentials. In the present calculations, the final self-consistent potentials are stable to within 0.005 Ry.

B. Tight-binding model

In this section a tight-binding model[20] for interacting p-like atomic states in a fcc lattice is described. This model will be used later to analyze the vacancy levels of the Si vacancy in the ideal crystal structure. We consider a fcc array of atoms which have three fold degenerate p-like atomic levels (P_x, P_y, P_z). Then Bloch functions of the form

$$\psi_1(\vec{k})=\frac{1}{\sqrt{N}}\sum_n e^{i\vec{k}\cdot\vec{R}_n}P_x(\vec{r}-\vec{R}_n) \ ,$$
$$\psi_2(\vec{k})=\frac{1}{\sqrt{N}}\sum_n e^{i\vec{k}\cdot\vec{R}_n}P_y(\vec{r}-\vec{R}_n) \ , \tag{9}$$
$$\psi_2(\vec{k})=\frac{1}{\sqrt{N}}\sum_n e^{i\vec{k}\cdot\vec{R}_n}P_z(\vec{r}-\vec{R}_n)$$

are constructed and the band structure $E_n(\vec{k})$ is given by diagonalizing

$$\begin{pmatrix} \langle\psi_1|H|\psi_1\rangle-E & \langle\psi_1|H|\psi_2\rangle & \langle\psi_1|H|\psi_3\rangle \\ \langle\psi_2|H|\psi_1\rangle & \langle\psi_2|H|\psi_2\rangle-E & \langle\psi_2|H|\psi_3\rangle \\ \langle\psi_2|H|\psi_1\rangle & \langle\psi_3|H|\psi_2\rangle & \langle\psi_3|H|\psi_3\rangle-E \end{pmatrix} , \tag{10}$$

where $\vec{k}$ is the wave vector, $\vec{R}_n$ are the lattice positions, and H is the crystal Hamiltonian. Assuming only nearest-neighbor interactions, the Hamiltonian matrix can be expressed in terms of three parameters: (a) u, the energy of the isolated atomic states, (b) σ, the interaction energy between parallel orbitals centered at neighboring atoms which point along the line connecting the atoms, and (c) π, the interaction energy between parallel orbitals centered at neighboring atoms which are perpendicular to the line connecting the atoms. Denoting $\vec{k}=(\xi_1,\xi_2,\xi_3)$ with ξ_i in units of $2\pi/a$ where a is the lattice constant of the fcc superlattice, the matrix elements are given by

$$\langle\psi_1|H|\psi_1\rangle=u+(\sigma+\pi)[\cos\pi(\xi_1+\xi_2)+\cos\pi(\xi_1-\xi_2)+\cos\pi(\xi_1-\xi_3)+\cos\pi(\xi_1+\xi_3)]+2\pi[\cos\pi(\xi_2+\xi_3)+\cos\pi(\xi_2-\xi_3)] \ ,$$
$$\langle\psi_2|H|\psi_2\rangle=u+(\sigma+\pi)[\cos\pi(\xi_2+\xi_3)+\cos\pi(\xi_2-\xi_3)+\cos\pi(\xi_2-\xi_1)+\cos\pi(\xi_2+\xi_1)]+2\pi[\cos\pi(\xi_3+\xi_1)+\cos\pi(\xi_3-\xi_1)] \ ,$$
$$\langle\psi_3|H|\psi_3\rangle=u+(\sigma+\pi)[\cos\pi(\xi_3+\xi_1)+\cos\pi(\xi_3-\xi_1)+\cos\pi(\xi_3-\xi_2)+\cos\pi(\xi_3+\xi_2)]+2\pi[\cos\pi(\xi_1+\xi_2)+\cos\pi(\xi_1-\xi_2)] \ ,$$

$$\langle\psi_2|H|\psi_1\rangle=(\pi-\sigma)[\cos\pi(\xi_1-\xi_2)-\cos\pi(\xi_1+\xi_2)] ,$$
$$\langle\psi_3|H|\psi_1\rangle=(\pi-\sigma)[\cos\pi(\xi_1-\xi_3)-\cos\pi(\xi_1+\xi_3)] ,$$
$$\langle\psi_3|H|\psi_2\rangle=(\pi-\sigma)[\cos\pi(\xi_2-\xi_3)-\cos\pi(\xi_2+\xi_3)] . \quad (11)$$

For some high-symmetry k points, the eigenvalues can be obtained easily without diagonalizing the 3×3 matrix, Eq. (10). At $\vec{k}=(0,0,0)$, $\langle\psi_i|H|\psi_i\rangle=u+4\sigma+8\pi$ and $\langle\psi_i|H|\psi_j\rangle=0$ for $i\neq j$. Therefore, the energies for the three bands are degenerate at Γ and have the energy

$$E(\vec{k}=\Gamma)=u+4\sigma+8\pi . \quad (12)$$

At $\vec{k}=X=(1,0,0)$ one has $\langle\psi_1|H|\psi_2\rangle=u-4\sigma$, $\langle\psi_2|H|\psi_2\rangle=u-4\pi$, $\langle\psi_3|H|\psi_3\rangle=u-4\pi$ and $\langle\psi_i|H|\psi_j\rangle=0$ for $i\neq j$. Thus two energy eigenvalues exist at X: one is singly degenerate

$$E_1(\vec{k}=X)=u-4\sigma , \quad (13)$$

the other is doubly degenerate

$$E_2(\vec{k}=X)=u-4\pi . \quad (14)$$

III. RESULTS AND DISCUSSIONS

A. Ideal structure

The first structural model used to study the electronic structure of a neutral Si lattice vacancy is the "ideal" structure. In this structure, the atoms surrounding the vacancy site remain in their crystalline positions after the vacancy is created. A portion of the Si crystal structure is shown in Fig. 2(a). Every Si atom is tetrahedrally coordinated and the valence electrons form covalent bonds linking the neighboring atoms. As a result of creating a vacancy, four bonds are broken [see Fig. 2(b)]. The electrons which previously participated in the broken bonds will tend to localize around the vacancy site and localized vacancy levels are expected to appear among the energy eigenvalues of bulk Si. In the present calculations, we have found both vacancy states deep in the Si thermal gap and strong resonant states embedded in the bulk bands.

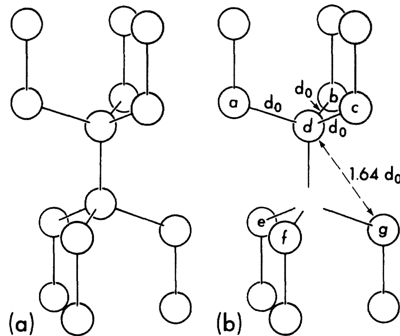

FIG. 2. Structure of cubic Si (a) and an undistorted Si lattice vacancy (b).

Before discussing the individual vacancy states, first the total, self-consistent valence charge density as given by the approximations discussed in Sec. II shall be examined. A necessary condition for the present calculations to represent noninteracting Si vacancies is that the charge density away from the vacancy site should closely resemble the charge density of bulk Si. Figure 3 displays the total valence charge density in a (110) plane for the ideal structure. The vacancy site is located at the center of the unit cell (open circle) and the atoms are indicated by full dots. Note that, for the center chain of atoms, both an atom and the associated covalent bonds are missing. The top and bottom chains are complete. Their charge densities are in good accord with densities obtained from bulk calculations[16,21] (which illustrates the local nature of the lattice perturbation).

As mentioned in Sec. I, vacancy levels which are dispersionless in $\vec{k}$ space for an isolated vacancy will appear as bands in the present periodic model. For the ideal structure, three vacancy bands in the Si thermal gap and one strong resonant band in the energy range of the valence bands are found. More weak resonant states corresponding to perturbed back bonds may exist in the valence bands. Figure 4 shows the energies of the vacancy bands at $\vec{k}=\Gamma$. The top figure depicts the positions of the $\vec{k}=0$ vacancy states with respect to the Si bulk density of states.[16] The three states in the gap are degenerate in energy at Γ. In the bottom figure, the energy levels at Γ for several runs in the self-consistent procedure are shown. The first row shows the energy levels of bulk Si in the 54-atom unit-cell structure. The empirical pseudopotential from Ref. 16 is used. There are 108 occupied valence bands separated from the conduction bands by the Si thermal gap (shaded area in Fig. 4). The second row shows the energy levels for the 53-atom unit cell (i.e., 53 Si atoms plus one vacancy) calculated using the empirical pseudopotential. The last row shows the energy levels for the 53-atom unit cell using the final self-consistent potential. The vacancy states are indicated by the arrows. Note that the final self-consistent vacancy levels appear significantly deeper in the forbidden gap than those calculated from the empirical pseudopotential. However, the energy of the resonant state at E

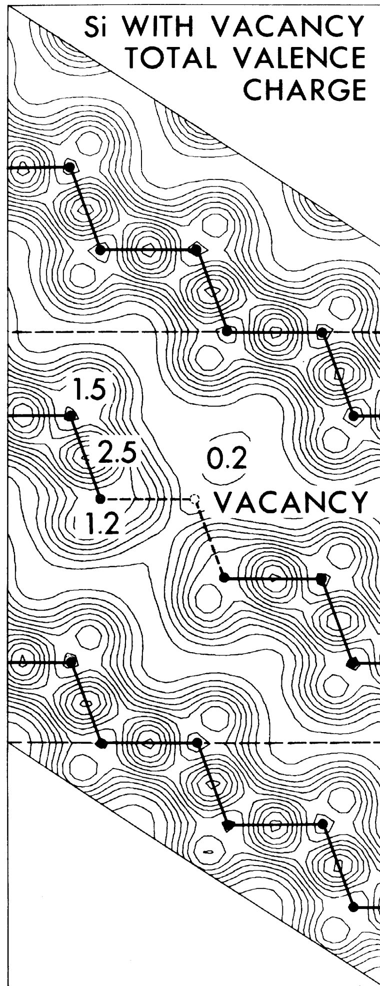

FIG. 3. Total, self-consistent valence charge density displayed in a (110) plane for a neutral Si vacancy in an ideal, unreconstructed structure. Charge values are normalized to one electron per unit cell which extends over 53 atoms and one vacancy.

~ − 8.2 eV is pinned in energy by the minimum of the density of states and changes only slightly in the course of achieving self-consistency.

In Fig. 5(a) the charge-density contour map for the vacancy states in the gap is displayed. The plotting plane is the same as in Fig. 3 [(110) plane] and the plotting area is enclosed by the two horizontal dashed lines in Fig. 3. As expected from the fact that these states appear deep in the gap, their charge density is fairly localized around the atoms surrounding the vacancy site. There is practically no charge built up on the atoms of neighboring chains, however, some charge overlap between vacancy states within the same chain is present. The charge distributions are dangling-bond-like, i.e., mostly p-like with a small mixture of s character. Figure 5(b) shows the charge-density contour plot for the resonant state in the valence band. Again the charge density is highly localized on the atoms surrounding the vacancy site. However, for this state, the charge distribution is mostly s-like around the atoms. Although these plots are calculated for states at Γ, they are representative for the vacancy states, since it is found that the charge distributions of the vacancy states are virtually identical for all $\vec{k}$ points in the fcc Brillouin zone.

The origin of the vacancy states can be understood using a simple molecular-orbital picture.[22] In this model, one assumes that in first order only the electrons in the broken bonds are significantly perturbed and that the wave functions of the vacancy states can be represented by a combination of atomic orbitals. Specifically, each molecular orbital (a single-electron vacancy state) is expressed as a linear combination of the dangling-bond orbitals (a,b,c,d) of the four atoms next to the vacancy site. Because of the symmetry of a Si vacancy in the ideal structure,

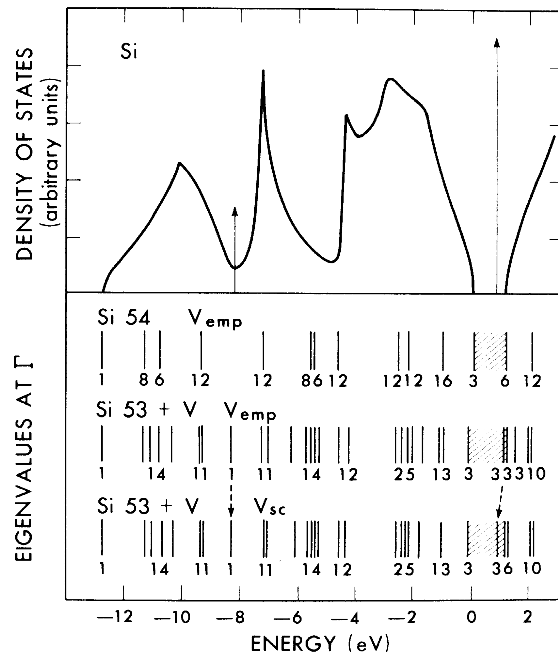

FIG. 4. (Top) crystalline density of states for Si with the position of strong resonant and vacancy levels at Γ. (Bottom) energies at Γ for the perfect 54-atom unit-cell crystal using an empirical pseudopotential, for the ideal vacancy using the same empirical pseudopotential and for the ideal vacancy using the final self-consistent pseudopotential are given. Note the lowering of the vacancy level in the fundamental gap.

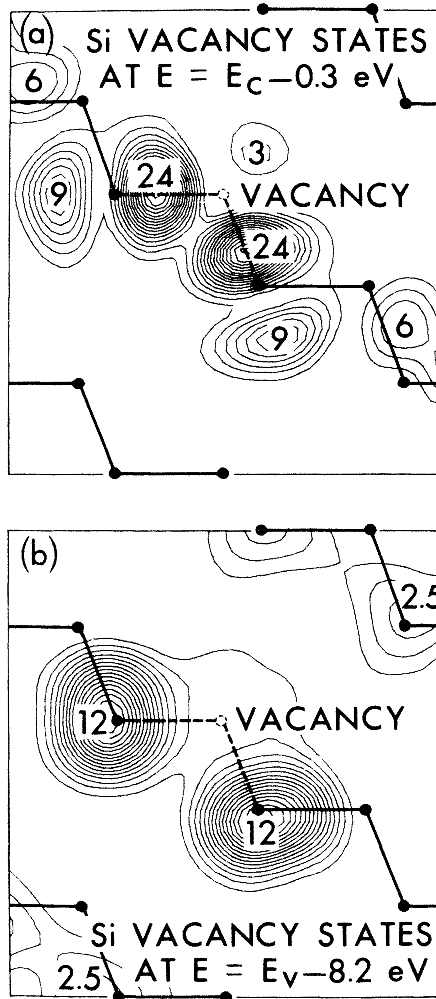

FIG. 5. Charge-density plots in a (110) plane (area enclosed by dashed lines in Fig. 3) of (a) the vacancy states in the fundamental gap and (b) the strong resonance around − 8.2 eV.

the molecular orbitals must transform under the operation of the group T_d according to irreducible representations of that group. Thus suitable single-electron wave functions are

$$\begin{aligned} v &= a+b+c+d \quad , \quad a_1 \\ t_x &= a+b-c-d \quad , \\ t_y &= a-b-c+d \quad , \quad t_2 \\ t_z &= a-b+c-d \quad . \end{aligned} \tag{15}$$

The resonant vacancy state at $E \sim -8.2$ eV has the symmetry of the state a_1, whereas the three states in the Si gap can be associated with the above t_2 states. This simple picture which correctly describes the symmetry of the vacancy states found, does not of course account for the dehybridization of sp^3 hybrids around the vacancy. The dehybridization into s-like and p-like states is, however, appreciable as seen from Fig. 5. Moreover, the simple model does not include possible resonant state owing to perturbed back bonds.

The dispersions of the vacancy states in $\vec{k}$ space which in a tight-binding picture are caused by the interactions between vacancies in the superlattice shall now be examined. The dispersion for the resonant vacancy state at $E \sim -8.2$ eV is found to be very small (~ 0.1 eV). This is confirmed by Fig. 5(b) in which virtually no overlap between orbitals centered at neighboring vacancy sites is found. However, the dispersion of the three vacancy states in the gap is appreciable which can be seen by the presence of charge between neighboring vacancy sites [see Fig. 5(a)]. This result indicates that the 54-atom unit cell chosen is not large enough to completely decouple the individual vacancies. In Fig. 6 symmetries and dispersions of the states in the gap along the Δ direction from Γ to X are shown schematically. In the ideal structure the three states are degenerate in energy at Γ with $E = 0.9$ eV. Along Δ, they split into one nondegenerate band (Δ_3) and one twofold degenerate band (Δ_5). At X the energy values are $E_2(X) = 0.7$ eV for the twofold degenerate states and $E_1(X) = -0.3$ eV for the nondegenerate state (all energies are given with respect to the valence-band maximum).

An estimation of the position of the energy levels for a single noninteracting vacancy is obtained using the tight-binding model described in Sec. IIB. Assuming that the dispersions of the vacancy bands in the Si gap are completely owing to nearest-neighbor interactions among the "p-like" single-electron vacancy states, the energy levels u for an isolated vacancy can be obtained by solving Eqs. (12)–(14) simultaneously. This yields the following expression for u:

$$u = \tfrac{1}{4}[E(\Gamma) + E_1(X) + 2E_2(X)] \quad . \tag{16}$$

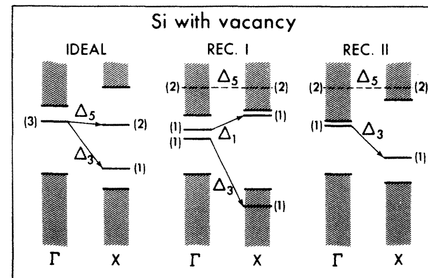

FIG. 6. Schematic energy diagram of dispersion between Γ and X and order of the Si vacancy levels in the fundamental gap as a function of different reconstruction models. For Rec I and Rec II, X is along the distorted [100] direction.

Using the calculated values for $E(\Gamma)$, $E_1(X)$, and $E_2(X)$, the energy for the threefold degenerate vacancy state in the gap for an isolated vacancy is $u = 0.5$ eV. At present no experimental data are available which allow comparison of this calculated value.

The radial dependence of the various one-electron potentials of interest for the ideal neutral Si lattice vacancy are displayed in Fig. 7. Nonspherical contributions to the potentials are negligibly small in the ideal structure. As described in Sec. II the self-consistent calculations are based on a lattice of Si^{4+} ionic potentials V_{ion} with one vacant lattice site (solid curve). The long-range Coulomb tail of this missing Si^{4+} ion is completely screened by the Hartree-exchange potential V_{HX} of four defect electrons (dashed line) as calculated from the total self-consistent valence charge distribution. The resulting vacancy potential V_{SC} (dotted line) is of short range similar to the empirical Si pseudopotential V_{emp} (dashed-dashed-dotted line) as used in crystal calculations. Compared to V_{emp}, however, V_{SC} shows a more repulsive core and a deeper well around 1 Å. A similar difference has been obtained in recent self-consistent surface calculations.[13] Also shown for comparison is the self-consistent pseudopotential V_{SC} (atom) obtained for an isolated atom by a calculation based on the same ionic Si^{4+} potential V_{ion} (dashed dotted curve). Even though the vacancy and the atomic potentials show comparable amplitudes for the repulsive core and the attractive bonding region, the self-consistent atomic potential is of considerably longer range and extends up to about 4 Å. This difference is due to the presence of covalent bonds in the crystalline case or dangling bonds in the vacancy case which lead to an increased electron density between 1 and 2 Å and thus to a stronger screening decreasing the effective range of the potential.

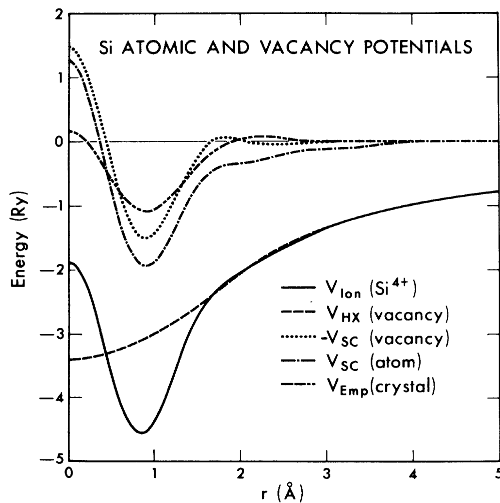

FIG. 7. Radial dependence of various Si atomic and vacancy potentials.

B. Reconstructed structures

Results presented in Sec. III A indicated that, in the ideal structure, there are three vacancy states in the Si thermal gap which are degenerate in energy. For a neutral vacancy, only one of the three states (neglecting spin) is occupied. This situation is unstable with respect to Jahn-Teller distortions[23] which lead to structural changes. Indeed, as discussed in Sec. I, the charged V^+ and V^- states for the Si vacancy are observed to undergo Jahn-Teller distortions which produce an uniaxial asymmetry in the electronic wave function along the cubic [100] direction. Although there exist no experimental data on the detailed structure of a neutral vacancy at present, it is generally believed that a similar type of distortion takes place for the neutral vacancy.

To study the effects of Jahn-Teller distortions on the vacancy levels, the electronic structure of a neutral vacancy is calculated for two differently reconstructed structural models. The first reconstructed structure is obtained by *shortening* the distance between atoms d and g and between atoms e and f in Fig. 2(b) by an amount equal to $\delta = 0.48 d_0$ where d_0 is the crystalline value of the Si-Si bond length. This is done by symmetrically moving the atoms toward each other along the connecting line. This type of distortion produces an asymmetry along the cubic [100] direction. The estimated value for δ is chosen to be in approximate agreement with the displacement found by Swalin[24] in his study of vacancy formation using Morse potentials. This value does not present an optimum choice, it merely represents a trial value. Figure 8 shows the total self-consistent charge density for this reconstructed structure (Rec I). As for the ideal case the charge density away from the vacancy is very much bulklike. However, the charge density near the vacancy site differs significantly from that obtained for the ideal structure. There appears bondlike charge between the two atoms which have been moved closer to each other, whereas the stretched back bonds become considerably weaker.

The effects of Rec I on the resonant vacancy level are small; its energy remains at ~ -8.0 eV. The effects of the distortion on the vacancy states in the gap, on the other hand, are significant. They are shown schematically in the center portion of Fig. 6. The threefold degeneracy at Γ is lifted by the uniaxial distortion. The lower band (labeled Δ_3) remains in the gap, whereas the twofold degenerate band (labeled Δ_5) merges

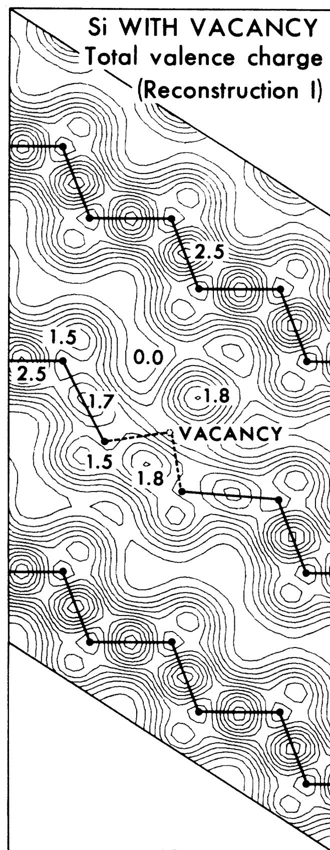

FIG. 8. Total self-consistent valence charge density for a neutral Si vacancy in a reconstructed environment (Rec I). The distances between the four atoms surrounding the vacancy are pairwise decreased, resulting in a [100] uniaxial distortion and a net relaxation *towards* the vacancy. Units are as in Fig. 3.

with the conduction band structure. The highest fully occupied band is now Δ_3, separated by a finite gap from unoccupied states indicating that no further symmetry reduction (i.e., Jahn-Teller distortion) is needed to stabilize the system. In addition, a *new* (empty) vacancy band, labeled Δ_1, appears in the gap. This state is induced by the chosen vacancy reconstruction and has its wave function localized at the vacancy site. Rec I has the net effect of moving the four atoms surrounding the vacancy site closer towards the vacancy site. This distortion stretches and weakens the back bonds. As a consequence some back-bonding charge is spread out and transferred to the second-nearest back bonds, which causes an increased vacancy-vacancy interaction in the present model. This effect is also recognizable from the increased dispersion of the Δ_3 vacancy band between Γ and X (see Fig. 6, middle). In analogy to the Si (111) surface, Rec I corresponds to an outward relaxation and therefore seems unlikely to occur.[25]

To study the effects of an opposite movement of atoms, another reconstructed structure, Reconstruction II (Rec II) is considered. The type and symmetry of distortions for this structural model is identical as for Rec I except for $\delta = -0.48d_0$, which corresponds to a contraction of back bonds and a net relaxation away from the vacancy site. Figure 9 shows the total, self-consistent charge density for Rec II. As compared to Fig. 8, charge has been removed from the immediate vacancy region and has been transferred into the back bonds.

As for Rec I, the distortion does not significantly affect the resonant vacancy level at about -8.0 eV. The behavior of the vacancy bands in the gap is shown on the right portion of Fig. 6. For Rec II, only one vacancy band (Δ_3) exists in the Si thermal gap. This band is fully occupied and separated by a finite gap from empty states. Thus, the type

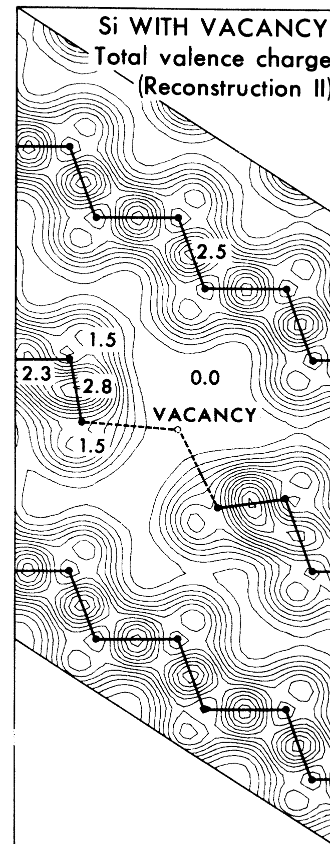

FIG. 9. Total self-consistent valence charge density for a neutral Si vacancy in a reconstructed environment (Rec II). Distances between the four atoms surrounding the vacancy are pairwise increased, resulting in a [100] uniaxial distortion and a net relaxation *away* from the vacancy. Units are as in Fig. 3.

of distortion of Rec II which lowers cubic symmetry leads to a Jahn-Teller stable situation. The strengthening of back bonds localizes the vacancy induced charge fluctuations which results in a decrease of dispersion of the vacancy bands along Δ (see Fig. 6). In contrast to Rec I, no empty vacancy state is found in the gap of Si. The Δ_5 vacancy levels become resonant levels with the conduction bands.

While the exact atomic positions of the reconstructed vacancy environment are still unknown, Rec II-type relaxations are expected to occur most likely. Analogies to the Si (111) surface relaxation[25] support this model. More experimental spectroscopic information about the neutral Si vacancy is needed to clarify the situation.

IV. CONCLUSIONS

The neutral lattice vacancy in Si has been studied embedded in a large 54-atom supercell using a self-consistent pseudopotential formalism. The method allows us to calculate self-consistently the response of valence electrons to an arbitrary arrangement of ionic cores. Thus three different structural models of the atoms surrounding the vacancy have been investigated. These models are: the ideal undistorted Si structure, (Rec I) a uniaxial [100] distortion with a net relaxation *towards* the vacancy site and (Rec II) a uniaxial [100] distortion with a net relaxation *away* from the vacancy site.

In each model one strong resonant virtually dispersionless band is found around -8.0 eV in the valence-band region. Its character is predominantly s-like on the four atoms surrounding the vacancy. In addition, vacancy bands appear in the fundamental gap, strongly influenced by the structural model used. In the ideal undistorted Si structure a threefold degenerate vacancy band is found with an estimated energy center of 0.5 eV above the valence-band edge. This level is onefold (neglecting spin) occupied which causes Jahn-Teller instabilities. Spin-resonant experiments on charged V^+ and V^- vacancies indicate the existence of a uniaxial [100] Jahn-Teller-type distortion, which can be assumed to also exist for the neutral vacancy. Both reconstruction models Rec I and Rec II result in a uniaxial [100] distortion. In both cases (inward and outward relaxation) *one* vacancy level is split away to lower energies resulting in a Jahn-Teller stable situation. Analogous considerations to the Si (111) surface relaxations favor model Rec II in which the four atoms surrounding the vacancy are relaxed away from the vacancy site, resulting in an increase in strength of back bonds. The studies presented here about the type of vacancy reconstruction existing in Si do not allow conclusive results and call for more experimental, spectroscopic information.

Part of this work was done under the auspices of the U.S. ERDA.

---

*Supported in part by the National Science Foundation Grant DMR72-03206-A02.

†Supported by a National Science Foundation fellowship.

‡Present address: Bell Laboratories, Murray Hill, N. J. 07974.

[1]A. B. Roitsin, Fiz. Tekh. Poluprovodn. 8, 3 (1974) [Sov. Phys.-Semicond. 8, 1 (1974)].

[2]F. P. Larkins, J. Phys. Chem. Solids 32, 965 (1971).

[3]F. P. Larkins and A. M. Stoneham, J. Phys. C 4, 143, 154 (1971).

[4]F. P. Larkins, J. Phys. C 4, 3065, 3077 (1971).

[5]R. P. Messmer and G. D. Watkins in *Radiation Damage and Defects in Semiconductors*, (Institute of Physics, London, 1972), No. 16, p. 255.

[6]D. Rouhani, M. Lannoo, and P. Lenglart, *International Conference on Radiation Effects in Semiconductors, Albany*, 1970, edited by J. W. Corbett and G. P. Watkins (Gordon and Breach, London, 1971), p. 15.

[7]J. Callaway and A. J. Hughes, Phys. Rev. 156, 860 (1967).

[8]G. D. Watkins, in *Proceedings of the Seventh International Conference on Physics of Semiconductors, Paris*, 1964, edited by M. Hulin (Academic, New York, 1965), Vol. 3, p. 97.

[9]J. A. Naber, C. E. Mallon, and R. E. Leadon, in *Proceedings of the International Conference on Radiation Damage and Defects in Semiconductors, Reading England*, edited by J. E. Whitehouse (Institute of Physics, London, 1973), p. 26.

[10]M. L. Cohen, M. Schlüter, J. R. Chelikowsky, and S. G. Louie, Phys. Rev. B (to be published).

[11]A superlattice of vacancies has been considered by Messmer and Watkins for vacancies in diamond in Ref. 5. They used the extended Hückel method and their calculation is not self-consistent.

[12]M. Schlüter, Kai Ming Ho, and M. L. Cohen (unpublished).

[13]M. Schlüter, J. R. Chelikowsky, S. G. Louie, and M. L. Cohen, Phys. Rev. Lett. 34, 1385 (1975); Phys. Rev. B 12, 4200 (1975).

[14]J. R. Chelikowsky, M. Schlüter, S. G. Louie, and M. L. Cohen, Solid State Commun. 17, 1103 (1975).

[15]S. G. Louie and M. L. Cohen, Phys. Rev. Lett. 35, 866; Phys. Rev. B (to be published).

[16]J. R. Chelikowsky and M. L. Cohen, Phys. Rev. B 10, 5095 (1974).

[17]M. L. Cohen and V. Heine, Solid State Phys. 24, 37 (1970).

[18]I. V. Abarenkov and V. Heine, Philos. Mag. 12, 529 (1965).

[19]See Ref. 13 for a detailed discussion of this problem which also occurs in surface calculations.

[20]J. C. Slater and C. F. Koster, Phys. Rev. 94, 1498 (1954).

[21]J. P. Walter and M. L. Cohen, Phys. Rev. B 4, 1877 (1971).

[22]G. D. Watkins and co-workers have used this type of simple picture to understand the EPR data on the Si vacancies.

[23]H. A. Jahn and E. Teller, Proc. R. Soc. A 161, 220 (1937).

[24]R. A. Swalin, Phys. Chem. Solids 18, 290 (1961).

[25]J. A. Appelbaum and D. R. Hamann, Phys. Rev. Lett. 32, 225 (1974); J. C. Phillips, Surf. Sci. 44, 290 (1974).